4. Physical phenomena in gas-phase synthesis

In synthesis in the gas phase, many phenomena play a role. The most important are:

- Homogeneous nucleation
- Condensation
- Collisions due to Brownian movement
- Coalescence due to solid state diffusion or viscous flow
- Surface reactions

These mechanisms are schematically shown in Fig. 4.1. Additionally, transport processes, e.g. due to thermophoresis or Brownian diffusion, play a role.

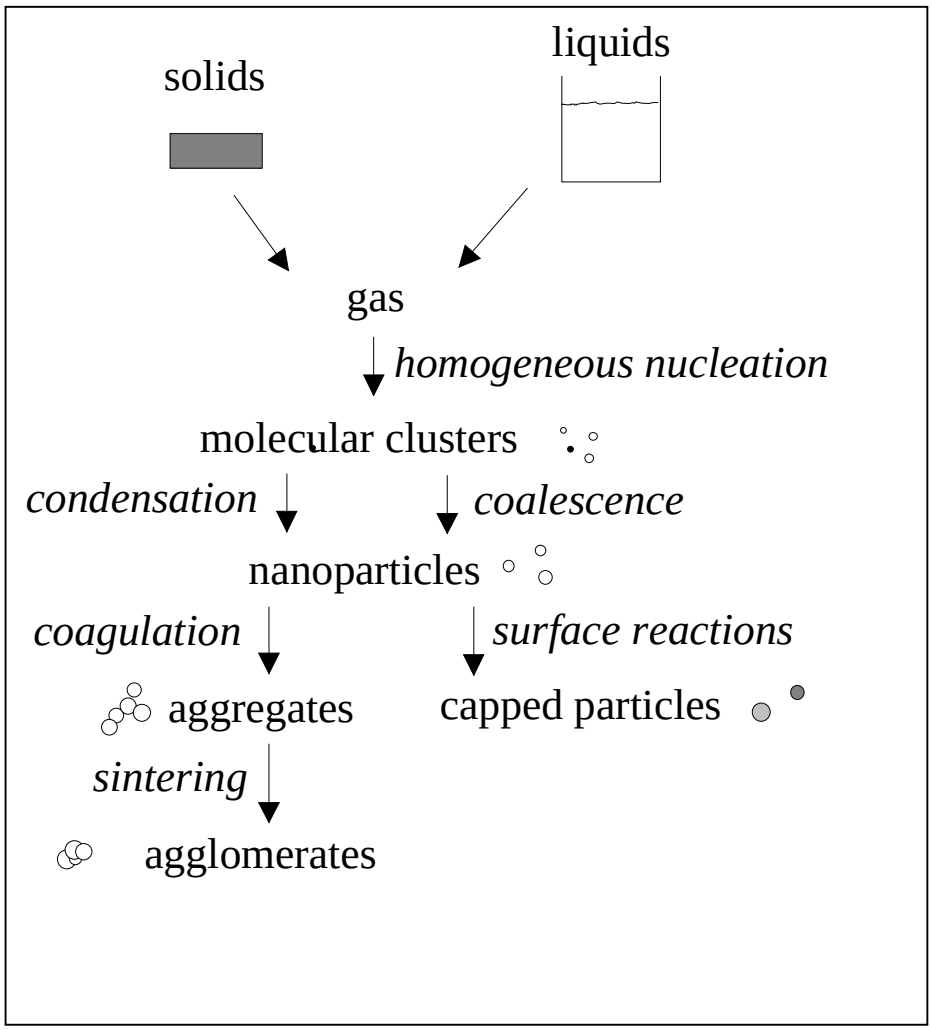

Fig. 4.1. Mechanisms in gas-phase nanoparticle synthesis

In this Chapter, several mechanisms related to relevant problems in the gas-phase synthesis of nanoparticles for functional applications are investigated. In

Chapter 4.1, the formation of nanometer-sized particles by the evaporation-condensation technique will be analyzed using a moment model describing nucleation, condensation and coagulation. This allows to predict the minimum furnace temperatures needed to form nanoparticles. The coagulation and aggregation phenomenon is modeled by a Monte Carlo simulation technique in order to be able to describe complex systems, such as multi-component or multidimensional systems with several variables, e.g. particle size and charge. The contents of Chapter 4.2 have been accepted for publication (Kruis *et al.*, 2000a). The method is useful for describing the mixing of charged nanoparticles for the synthesis of composite nanoparticles (Chapter 4.3).

4.1 Particle formation by nucleation, condensation and coagulation: application to synthesis in tube furnaces

Most of synthesis methods for gas phase nanoparticle synthesis are formation are still in the laboratory stage, and process design and product development rely heavily on experience. Aerosol science provides a theoretical framework for understanding particle formation processes in the gas phase, which can be used to understand experimental results or to find favorable process conditions. Modeling of most aerosol reactors is very complex due to the interplay of many physicochemical phenomena and due to the problematic description of complex phenomena such as exploding wires and laser evaporation of solid material. Therefore, a gas which is heated and subsequently rapidly cooled down is chosen here as a model system. In this so-called evaporation-condensation process (Scheibel and Porstendörfer, 1983), a saturated vapor is cooled resulting in a supersaturation, thereby producing nanosized particles. The same basic phenomena occur in the more complex systems as laser ablation and inert-gas condensation but there the process conditions are not so easily defined.

Several approaches for modeling particle formation in tube furnaces have been described in the literature. Panda and Pratsinis (1995) assume a monodisperse size distribution to describe the formation of aluminium particles in a furnace. A more detailed model describes the changes in the first three moments of the particle size distribution due to nucleation and condensation (Friedlander, 1983). This allows to assume a lognormal particle size distribution. In order to close these three moments, Pratsinis (1988) assumed a lognormal size distribution and added the coagulation mechanism. More advanced modeling techniques do not assume a shape of the particle size distribution but require longer computation times and more complexe numerical methods.

In this subchapter, particle formation in tube furnaces is analyzed using a moment model, based on Pratsinis (1988) but modified for the non-isothermal conditions of tube furnaces. After validation of the model, most of the chemical elements have been screened in order to find conditions necessary for nanoparticle synthesis using the evaporation-condensation mechanism in tube furnaces.

4.1.1 Theory

In the evaporation-condensation process, a vapor is generated by slow evaporation or sublimation of a powder material in an evaporation boat and can form particles by homogeneous nucleation when cooling down. In order to calculate the supersaturation the saturation vapor pressure is described in terms of the general equation:

$$\log p_s = \frac{A}{T} + B \log T + C\,T + D\,T^2 + E \tag{4.1.1}$$

This expression is fitted to the experimental data (Honig and Kramer, 1969) for most of the elements. The expression proposed by Girshick and Chiu (1990) for the homogeneous nucleation rate is used here:

$$I = v_1 \sqrt{\frac{2\gamma}{\pi m_1}}\, n_s^2\, S \exp\left(\theta - \frac{4\theta^3}{27(\ln S)^2}\right) \tag{4.1.2}$$

using the dimensionless surface tension group θ:

$$\theta = \frac{\gamma s_1}{k_B T} \tag{4.1.3}$$

A linearly temperature-dependent surface tension (Mezey and Giber, 1982) is used in this work. The supersaturation S is found using:

$$S = \frac{\hat{n}_1 \rho_g}{n_s} \tag{4.1.4}$$

the number of monomers in the particles formed by homogeneous nucleation is:

$$k^* = \left(\frac{2\theta}{3\ln S}\right)^3 \tag{4.1.5}$$

The particle dynamics can be described in terms of the three leading moments of the size distribution, approximating the form of the distribution as lognormal:

$$n(v,t) = \frac{1}{3\sqrt{2}\ln\sigma}\exp\left(-\frac{\ln^2\left(v/v_g\right)}{18\ln^2\sigma}\right)\cdot\frac{1}{v} \qquad (4.1.6)$$

The moments M_0, M_1 and M_2 are related to the geometric average particle volume v_g and the standard deviation σ by:

$$M_k = M_0 v_g^k \exp\left(\frac{9}{2}k^2\ln^2\sigma\right) \qquad (4.1.7)$$

Following Pandas and Pratsinis (1995) the moments and the monomer concentration are expressed per unit mass of carrier gas instead of using concentrations per unit volume of carrier gas. This is done in order to cope with the non-isothermal conditions in the system. We define:

$$\hat{M}_k = \frac{M_k}{\rho_g} \qquad (4.1.8)$$

this transforms the moment equation into:

$$\frac{\mathrm{d}\hat{M}_0}{\mathrm{d}t} = \frac{I}{\rho_g} + \left(\frac{\mathrm{d}\hat{M}_0}{\mathrm{d}t}\right)_{coag} \qquad (4.1.9)$$

$$\frac{\mathrm{d}\hat{M}_1}{\mathrm{d}t} = \frac{I\,k^* v_1}{\rho_g} + \left(\frac{\mathrm{d}\hat{M}_1}{\mathrm{d}t}\right)_{cond} \qquad (4.1.10)$$

$$\frac{\mathrm{d}\hat{M}_2}{\mathrm{d}t} = \frac{I\left(k^* v_1\right)^2}{\rho_g} + \left(\frac{\mathrm{d}\hat{M}_2}{\mathrm{d}t}\right)_{coag} + \left(\frac{\mathrm{d}\hat{M}_2}{\mathrm{d}t}\right)_{cond} \qquad (4.1.11)$$

in which the change of the moments due to a specific mechanism (nucl=nucleation, cond=condensation, coag=coagulation) is a function of the moments themselves, derived by Pratsinis (1986). Harmonic averaging is being applied in order to cope with the different coagulation and condensation rates in the free-molecular and continuum regime. The monomer mass balance, also expressed per unit mass carrier gas, is:

$$\frac{\mathrm{d}\hat{n}_1}{\mathrm{d}t} = -\frac{Ik^*}{\rho_g} + \left(\frac{\mathrm{d}\hat{n}_1}{\mathrm{d}t}\right)_{cond} \qquad (4.1.12)$$

The gas density, gas viscosity and mean free path of the gas are described using temperature-dependent functions.

4.1.2 Results and discussion

Until now, no systematic study of the nucleation behaviour of the elements has been carried out. It is, however, very useful to know which temperatures are needed to induce particle formation. Applying the homogeneous nucleation formula, the following screening procedure is used. At a certain maximum temperature, which can be thought of as the furnace temperature for instance, a monomer concentration is generated in accordance with the saturation pressure. Then the gas is cooled and supersaturation is created. The nucleation rate has to be screened over the whole range between maximum temperature and room temperature, as it is possible that a system shows no nucleus formation (here defined where the nucleation rate is smaller than 1 cm^{-3}/s, which is an often encountered criterion for particle formation) at room temperature but it does at intermediate temperatures. B, C, W, Cr, Ge and Si e.g. show this behaviour. This can be seen in Fig. 4.1.1 which shows the nucleation rate of several elements when initially a temperature of 60 % of the melting point is established and then cooled down to the indicated temperature. This maximum in the nucleation rate is however an exception, usually a continuously increasing nucleation rate is found when going to lower temperatures.

The moment method was applied to follow the complete particle formation process with nucleation, condensation and coagulation. In order to validate the model, experimental results for silver nanoparticles (Scheibel and Porstendörfer, 1983) are modeled. In these experiments, silver powder in a boat is heated in a tube furnace, forming nanoparticles during the cooling down. The temperature and cooling rate was determined experimentally and the particle size distribution was measured using a DMA. The temperature at the center of the tube was found to be 70 K lower than the furnace temperature. In Fig. 4.1.2 it can be seen that the model describes the experiments (which apply a cooling rate of 3300 K/s) satisfactorily, in view of the incertainties in the surface tension and the nucleation model. The influence of the cooling rate is also shown: the higher the cooling rate, the smaller the resulting particle size at a given temperature. This can be explained from the competition between nucleation at the one hand and condensation and coagulation at the other hand. A slow cooling down results in a lower nucleation rate, so that the particles formed have more time for interaction which each other and with condensing molecules.

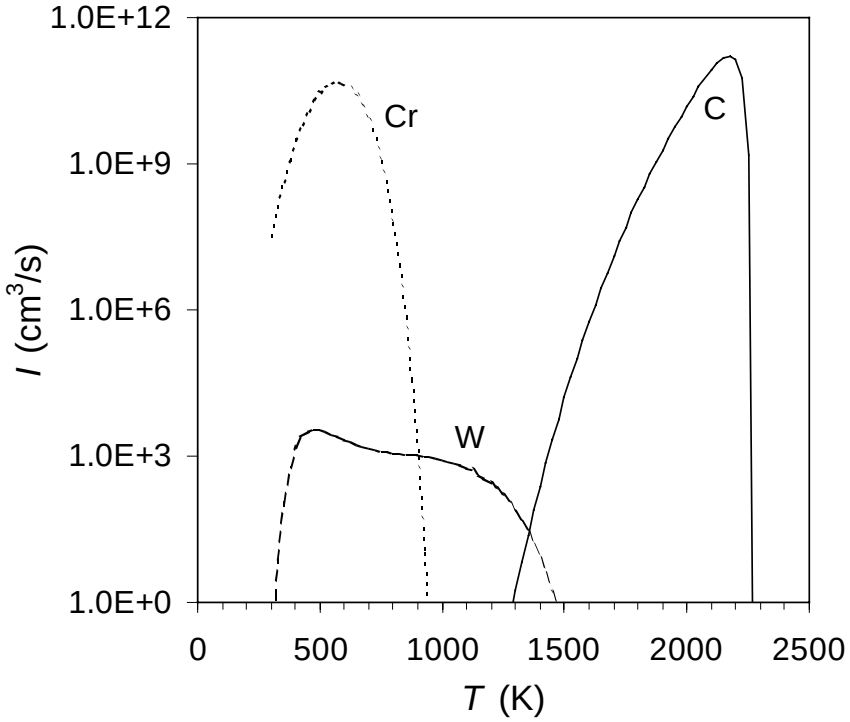

Fig. 4.1.1. Nucleation rate of different elements in N_2 at 1 bar as function of temperature, after creating saturation at T=0.6 T_m (2294 K for C, 2210 K for W, 1278 K for Cr)

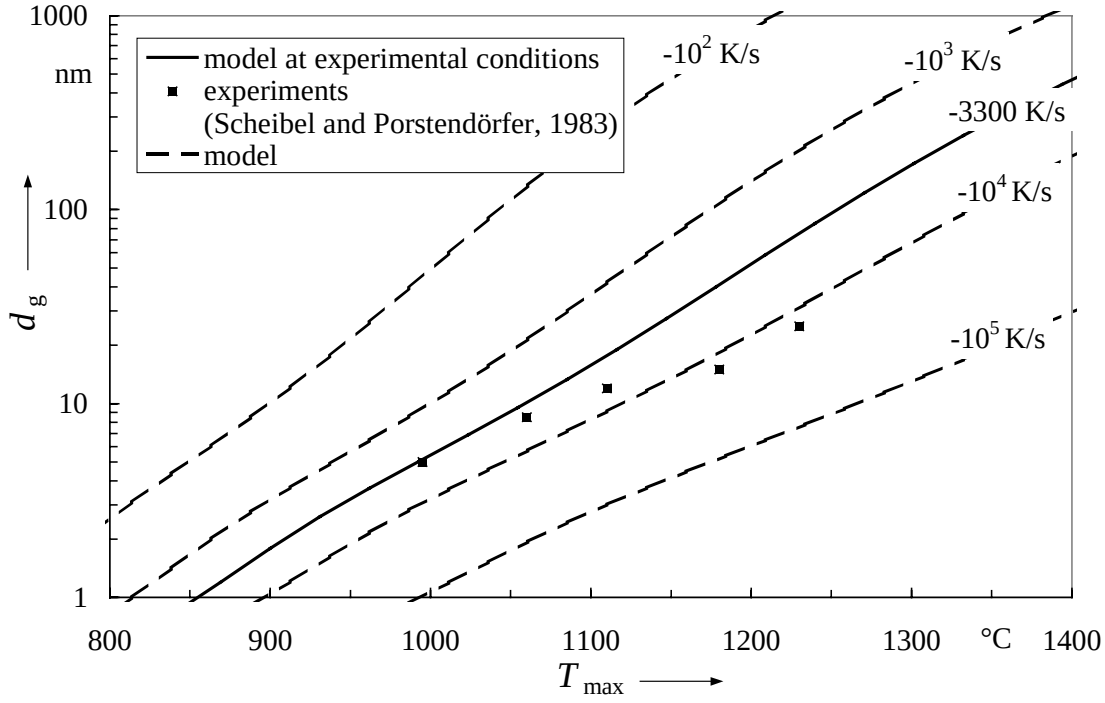

Fig. 4.1.2. Geometric mean particle diameter of Ag particles when cooling down from T_{max} to room temperature with different cooling rates indicated. Lines are based on the moment model, experimental data is shown as points.

The nucleation model and the moment model are now used to screen the different elements on their ability to form nanoparticles. Here we distinguish nucleation ability and particle formation ability. In table 1 it can be seen to what temperatures a material has to be heated to initiate nucleus formation, indicated by T_n. As can be seen, almost all elements show initial particle formation when heated up to the melting point. The results are independent of system pressure or carrier gas, as the saturation pressure is pressure-independent. It has to be pointed out that the surface tension is a very critical parameter in calculating the nucleation rate. Small changes in the surface tension lead to dramatic changes in the nucleation rate. Therefore the table should be viewed with some care. The other way around, nucleation experiments could be used to check the correctness of the applied surface tension.

The next question is to what particle size the nuclei will grow when nucleation occurs. Using the standard submicron particle detection techniques such as condensation nucleus counters particles as small as 3 nm can be detected. For the elements shown in Table 4.1, the moment model was applied in order to find the maximum temperature needed resulting in a geometric particle diameter of 3 nm. This temperature is indicated in the table by T_p. A cooling rate of 10^3 K/s was chosen which is a normal cooling rate to be expected in tube furnaces. Rates in the order of 10^5 K/s are more characteristic for plasma- and laser-driven syntheses. The calculation has been performed until the temperature reaches room temperature.

As can be seen from the table, is this temperature T_p in most cases hundreds degrees Kelvin higher than the maximum temperature where the nucleation starts. Thus it seems that this ‘nucleation’ criterion expressed by T_n is not a practical criterion in order to predict the start of detectable particle formation. The table can be used in order to get an idea of the minimum furnace temperatures needed for nanoparticle formation of the different elements.

From this table, also the limitations of the evaporation-condensation method using tube furnaces become clear: the temperature needed for nanoparticle formation is for many elements above 2000 K, so that the use of tube furnaces becomes questionable due to material problems and too elevated costs. An example of such an element is Pt, which is potentially interesting as dopant in gas sensing applications. For these elements, alternative methods have to be applied which are crucible-free, such as laser ablation.

Table 4.1. Melting temperature T_m, maximum temperatures necessary for nucleus formation T_n ($I > 1$ cm^{-3}/s) and maximum temperature T_p needed for reaching a geometric particle diameter of 3 nm. For the calculation of T_p, a cooling rate of 10^3 K/s until room temperature was used with N_2 at atmospheric pressure as carrier gas.

	T_m/K	T_n/K	T_p/K		T_m/K	T_n/K	T_p/K		T_m/K	T_n/K	T_p/K
Ag	1235	740	1190	K	337	380	430	Ru	2583	1550	2330
Al	934	840	1310	La	1193	1120	1740	S	386	310	360
As	1267	480	560	Li	454	450	690	Sb	904	490	720
Au	1338	960	1530	Mg	922	610	660	Sc	1812	940	1410
B	2573	1440	2110	Mo	2890	1620	2490	Se	490	320	460
Be	1551	840	1300	Mn	1517	730	1120	Si	1683	1080	1620
Bi	545	530	840	Na	371	390	490	Sr	1042	480	690
C	3823	1760	2450	Nb	2741	1810	2630	Ta	3269	1900	2940
Ca	1112	530	760	Ni	1726	1210	1590	Tc	2445	1610	2450
Co	1768	1130	1660	Os	3318	1860	2850	Te	723	390	580
Cr	2130	980	1530	P	317	310	420	Ti	1933	1120	1740
Cu	1357	790	1250	Pb	601	550	870	Tl	577	590	800
Fe	1808	1010	1590	Pd	1825	950	1530	U	1406	1180	1740
Ga	303	720	1150	Po	527	360	530	V	2163	1210	1860
Ge	1211	820	1260	Pt	2045	1350	2130	W	3683	1990	3020
Hf	2500	1950	2950	Rb	312	360	390	Y	1796	1040	1620
In	430	450	560	Re	3453	1865	2900	Zn	693	570	600
Ir	2638	1790	2480	Rh	2239	1300	2060	Zr	2125	1450	2340

4.2 Coagulation and aggregation: a Monte Carlo simulation

Once particles are formed and are solid, coalescence will not any more be rapid and aggregates consisting of primary particles develop. When the collision takes place at room temperature, in general the primary particles will conserve their original shape. At higher temperatures, solid state diffusion or viscous flow between the primary particles can lead to complicated structures.

The classical way of dealing with coagulation (here defined as describing colliding droplets) and aggregation (describing colliding solid particles) is the Smoluchowski equation (Smoluchowski, 1917). An analytical solution to this equation is only possible in the case of simple collision kernels, which are not relevant for the

systems of interest discussed above. In the case of complex coagulation kernels however, the problem has to be solved by numerical means.

This population balance problem is traditionally solved by discrete population balances, moment methods or sectional methods. Solving the discrete particle (or ’cluster ‘) dynamic equation based on the Smoluchowski equation for the whole submicron size spectrum implies that more than 10^9 differential equations have to be solved simultaneously in order to describe the particle size distribution $n(v,t)$ between 1 nm and 1 µm. This is computational too expensive at the moment. It has been done, however, for only a small part of the particle size spectrum, e.g. up to 20 basic units in a particle whereas the larger particles are described by the sectional representation (Landgrebe and Pratsinis, 1990). Another way of numerical simulation assumes some form of the particle size distribution, e.g. a log-normal one, which results in a few relatively easy to solve equations for the moments of the distribution (Pratsinis, 1988, Otto and Fissan, 1999). Finally, the particle size distribution can be cut into sections for which differential equations can be derived (Litster *et al.*, 1995). It provides the solution accurately when the number of sections is high enough with a reasonable computational time.

All these methods have the following drawbacks:

- There is no information about the history of each particle. The particles are described by means of their volume. It cannot be traced back which particles collided to form a bigger particle and the information about the internal structure is lost. Especially in case of aggregates this is a problem, as sometimes the size distribution of the primary particles composing an aggregate has to be known. Such cases are e.g. the mixing of solid particles with different composition and the coating of large particles with smaller ones.
- When more-dimensional systems have to be dealt with, the sectional representation results in very complex algorithms. Examples are additional information about the agglomerate form (Xiong and Pratsinis, 1993) using a particle size distribution $n(v,a,t)$ describing the particle volume and area or about the charge distribution (Vemury *et al.*, 1997) which requires the solution of $n(v,q,t)$ describing volume and charge level.

A classical method to overcome such drawbacks is to use Monte Carlo simulation methods. A well-known example of this method is the simulation of the Brownian movement by stochastic processes. When a sufficient number of particles is taken, collisions will result from the random Brownian motions and a change in the particle size distribution can be recorded. With the help of such trajectory methods based on the Langevin equation Brownian coagulation of droplets (Pearson *et al.*, 1984) and agglomerate formation by Brownian coagulation (Gutsch *et al.*, 1995) have been described. Such methods can deliver a priori coagulation rates, but are time-consuming

and are not suited for simulating large number of particles. The number of simulated particles is here usually between 500 and 1000.

When the collision rates are known, a much simpler method can be used. This method bases on choosing collision partners by a stochastic game and is known as the Direct Simulation Monte Carlo method (DSMC, Bird, 1976). It was originally developed for describing gas dynamics and is essentially the simulation of molecular collisions without regarding their spatial positions. As the number of particles in real systems is too large for the present computer memories, the simulation volume is chosen such that a reasonable amount (10^4 – 10^5) of simulation particles results. Advantageous is that information about the history and internal structure of the particles is available, and that multi-dimensional systems such as charged and multicomponent aerosols, requiring the solution of $n(v,q,c,t)$ describing particle volume, charge level and composition, can be simulated. Monte Carlo (MC) simulations are computationally expensive, computer power has reached however a level where simulations with up to 10^5 particles are now possible on fast PCs. Furthermore, more care has to be taken to ascertain that the numerical solutions, which vary due to the use of random numbers, are representative ones. The MC algorithms for solving particle dynamics are however easily programmed, and it can be said that in comparison to sectional models the time spent on solving a problem is shifted from the programmer to the computer.

The DSMC method has been used before to solve complex problems which involved particle collisions (e.g. Shah *et al.*, 1977, Bapat *et al.*, 1983). There are however few studies in which different DSMC methods for solving the coagulation and aggregation problem are investigated and tested more in detail. In this subchapter, these methods are briefly described and then a related method is proposed which is computationally more efficient. The accuracy of the solutions is tested by comparing them with (I) analytical solutions and (II) numerical results from a sectional model. Two examples of industrial relevance are given to show the suitability of the DSMC method for describing complex multi-dimensional particle dynamics.

4.2.1 Direct Simulation Monte Carlo methods

It is assumed that the *N* colliding particles with an initial distribution $n_0(v)$ are contained in a fluid of volume *V*. This volume is chosen such that *N* is a reasonable number, with the present personal computer power not more than 10^5. It is further assumed that all collisions are binary, i.e. we are not dealing with concentrated dispersions or slurries, and that the sticking coefficient is unity. The collision rate β is a known function which depends on the properties of the medium and on the properties of the colliding particles.

The particulate system considered here is usually described by the Smoluchowski equation:

$$\frac{\partial n_k}{\partial t} = \frac{1}{2}\sum_{i=1}^{k-1} \beta_{i,k-i} n_i n_{k-i} - n_k \sum_{i=1}^{\infty} \beta_{i,k} n_i \qquad (4.2.1)$$

where t is the time, n_k is the number concentration of the k-fraction and $\beta_{i,k}$ is the collision rate of the particle pair (i,k) which defines the kinetics of the process. In the DSMC method, particle pairs are selected by stochastic methods based on the transformation of collisions rates into collision probabilities.

Garcia *et al.* (1987) describes two stochastic methods based on the simulation procedure for a Markov process. The methods were not tested by these authors, however. The mean time between two collisions events is τ, which can be calculated by:

$$\tau = \frac{1}{\sum_{i=1}^{N}\sum_{j=i+1}^{N} \beta_{i,j}^{V}} \qquad (4.2.2)$$

in which β^V is the collision rate in a volume V. It is assumed that τ is an exponentially distributed random variable. This time is therefore selected by means of a random number generator. The coagulation pair (i,j) is chosen on the basis of the probability $Pr_{i,j}$ which is calculated by:

$$Pr_{i,j} = \frac{\beta_{i,j}^{V}}{\sum_{k=1}^{N}\sum_{l=k+1}^{N} \beta_{k,l}^{V}} \qquad (4.2.3)$$

As it is in this method necessary to calculate the collision rates of all possible particle pairs (inverse method) which is time-consuming, Garcia *et al.* (1987) proposed a second method based on the acceptance-rejection procedure (Bird, 1976). Here, a particle pair (i,j) is selected entirely at random independent of the collision probability. Then this pair is accepted as a collision pair if

$$R < \frac{\beta_{i,j}^{V}}{\max\left\{\beta_{k,l}^{V}\right\}} \qquad (4.2.4)$$

where R is a random number uniformly distributed between 0 and 1. When the pair is rejected, a new random number is selected, and so on, until the condition is fulfilled. This method is only practical when the maximum of the collision rate can easily be

determined and might introduce an error according to Garcia *et al.* (1987). In order to investigate this error, simulations are compared based on this method with the analytical solution for the simple collision kernel $\beta = A(i + j)$ (described further in this subchapter). The results are shown in Fig. 4.2.1. Even with 10^5 simulation particles, the error in the total particle number is rather large as in comparison with the results which will be shown further on. Furthermore, when the range of particle sizes increases the ratio of the randomly generated collision rate and the maximum collision rate becomes very small, the large number of rejections slows down the program considerably. As an example, in an aerosol system with wide range of particle classes undergoing Brownian coagulation $\beta(d_1 = 1\,\text{nm}, d_2 = 1\,\text{nm}) / \beta(d_1 = 1\,\text{nm}, d_2 = 100\,\text{nm})$ at standard conditions is in the order of 10^{-3}.

A third method is proposed by Liffman (1992) who uses a two-step method. The mean time which particle *i* experiences between two collision events is:

$$\tau_i = \frac{1}{\sum_{j=1}^{N} \beta_{i,j}^{V}} \qquad (4.2.5)$$

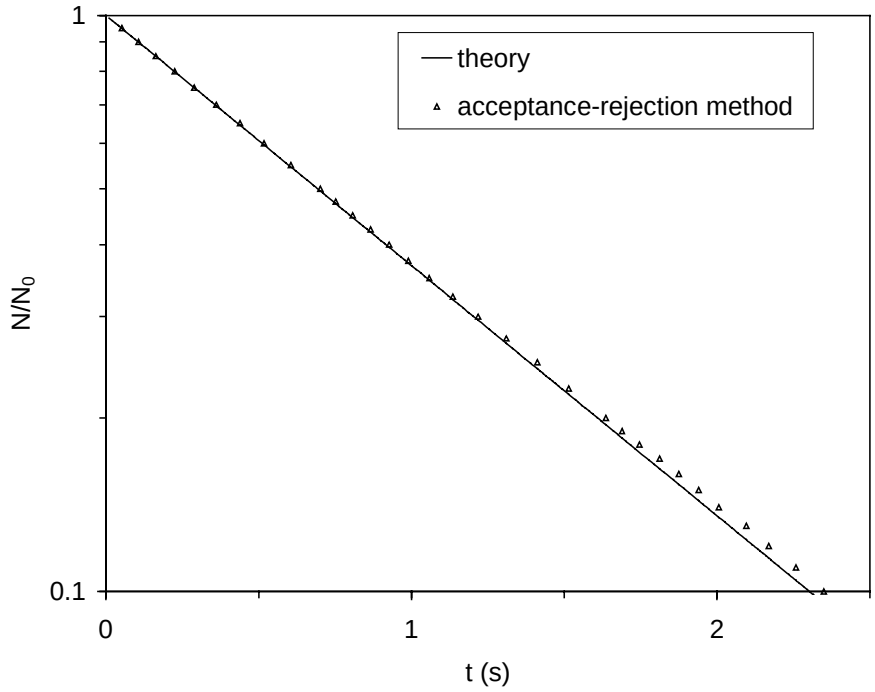

Fig 4.2.1. Decrease in relative total number concentration N / N_0: comparison between theory (Case 2 , $\beta_{i,j}$=A(i+j)) and the acceptance-rejection Monte Carlo simulation procedure of Garcia et al. (1987). Number of simulation particles: 10.000

It is assumed that this time is an exponentially distributed function. A time step is chosen which should be much smaller than the smallest value of all possible τ_i's. Then, the particle *i* is accepted if

$$R < 1 - e^{\left(-\frac{\Delta t}{2\tau_i}\right)} \tag{4.2.6}$$

When *i* has been found, the collision partner *j* is found by computing first all collision probabilities between the chosen particle *i* and any other particle *j*:

$$Pr_j = \frac{\beta_{i,j}^V}{\sum_{k=1}^{N} \beta_{i,k}^V} \tag{4.2.7}$$

and then selecting *j* by means of:

$$\sum_{k=1}^{j-1} Pr_k \le R \le \sum_{k=1}^{j} Pr_k \tag{4.2.8}$$

As in the acceptance-rejection method of Garcia *et al.* (1987), selecting one particle pair might take a large number of random numbers which is computationally expensive. A further problem is that it is no clear criterion to select the time step. Nevertheless, the simulation results were extensively compared with analytical solutions and found to be correct.

4.2.2 A Fast DSMC method

A new method is proposed which is related to the inverse method. As the collision kernel represents the probability of a binary collision in unit time, the sum over all collision kernels will be the probability that one collision takes place in the particle ensemble in unit time. So the mean time $\langle\tau\rangle$ needed for one collision taking place in the particle ensemble is the inverse of the sum of all collision kernels:

$$\langle\tau\rangle = \frac{2}{\sum_{i=1}^{N} \sum_{i=1, i\neq j}^{N} \beta_{i,j}^V} \tag{4.2.9}$$

The factor 2 is added in order to account for the double counting of the particle pairs. A collision pair is chosen by making a list of all pairs and accumulate the collision rate until the sum surpasses a random number. If a random number *R* is

uniformly distributed in (0,1], $R\sum\sum\beta_{i,j}^{V}$ is uniformly distributed in (0, $\sum\sum\beta_{i,j}^{V}$]. We can put the selection criterion as follows:

$$\sum_{k=1}^{i}\sum_{l=1}^{j}\beta_{k,l}^{V} \le R\sum_{k=1}^{N}\sum_{l=1}^{N}\beta_{k,l}^{V} \le \sum_{k=1}^{i}\sum_{l=1}^{j+1}\beta_{k,l}^{V} \quad \text{with } k \neq l \tag{4.2.10}$$

which causes the particle pair *(i,j)* to form a new particle with volume $v_i + v_j$ (see Fig. 4.2.2). Only one random number is used for the selection of a particle pair and no acceptance-rejection procedure takes place. If *m* steps are completed, the total time can be simply calculated from:

$$t = \sum_{i=1}^{m}\langle\tau\rangle_i \tag{4.2.11}$$

When an initial size distribution has to be modeled, it is generated by means of a random generation method (Rubinstein, 1981). The DSMC method can be applied in a aggregation mode, in which each aggregate is assigned an array indicating which primary particles compose the aggregate, or in an coagulation mode, in which after each collision the new (droplet) properties such as volume and density are stored.

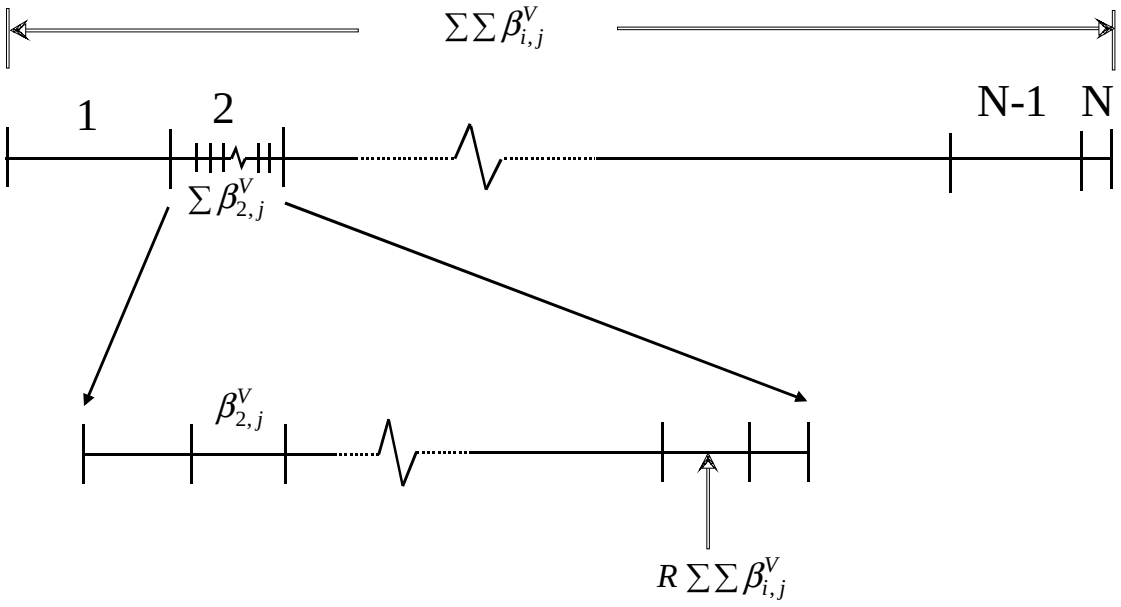

Fig. 4.2.2. Illustration of the MC technique used to choose pairs of colliding particles (i,j) by means of a random number R. In this procedure the collision rates of all possible particle pairs are weighted.

During the simulation the number of simulation particles N drops, which means that the error increases as the sample error is in the order of $\sigma/\sqrt{N}$. In order to encounter this, the simulation volume V and the number of particles N are doubled when the concentration has dropped by half. The properties of each 'old' particle are of course copied to the 'new' particles in the additional volume in order to conserve the statistical properties. This procedure is discussed by Liffman (1996).

It should be pointed out that this method necessitates the calculation of the collision rates of all possible particle pairs. If N is large, the storage of N^2 collision rates becomes prohibitive: 10^5 simulation particles would mean the storage of 10^{10} collision rates. In order to overcome this, for each particle only the sum of possible collision rates is stored and by means of the random number it is determined which particle i is selected. Then the collision rates of i with the other particles is calculated and summated until the condition 10 is met. This method implies the storage of only N values. After each pair selection, a simple correction can be made in the summated collision rate values to account for the change in particle properties and, consequently, in the collision rates. The large number of calculations of the collision rate, which are independent of each other, makes the simulation very suitable for parallel computing.

The method described here is similar to the inverse method of Garcia *et al.* (1987). However, exponentially distributed time steps between collisions which would necessitate a random number and a correction of all collision rates as in the work of Garcia are not used, instead a calculated deterministic mean time is used. This is possible due to the large number of simulated particles and greatly accelerates the simulation procedure.

4.2.3 Comparison with theoretical solutions for aggregation

Obviously, the fast DSMC must be compared to known theoretical solutions to determine if it is a valid method of analysis and to become an idea of the accuracy. There exist only a few forms of the collision kernel for which an analytical solution of the Smoluchovski equation exists (Spouge, 1983). $\beta_{i,j}=A$, $\beta_{i,j}=A(i+j)$, $\beta_{i,j}=Aij$. Here A is a constant, i,j are the section numbers. The fast DSMC method is examined using these collision kernels. The initial particle size distribution is monodisperse.

Case 1. $\beta_{i,j}=A$. If we define N_0 as the initial number of primary particles at $t=0$, the total number of particles N at time t is

$$N=\frac{N_0}{1+N_0At/2} \qquad (4.2.12)$$

The probability of obtaining a particle, containing k primary particles is:

$$P_k = \frac{(N_0 At/2)^{k-1}}{(1+N_0 At/2)^k} \qquad (4.2.13)$$

Case 2. $\beta_{i,j}=A(i+j)$. In this case the decrease of particle number can be expressed as:

$$N = N_0 e^{-N_0 At} \qquad (4.2.14)$$

with the probability of obtaining a k-aggregate

$$P_k = \frac{k^{k-1}}{k!}(1-e^{-N_0 At})^{k-1} e^{-k(1-e^{-N_0 At})} \qquad (4.2.15)$$

Case 3. $\beta_{i,j}=Aij$. In this case there exists only an analytical solution for times shorter than a finite time $t=1/N_0A$,

$$N = N_0(1-N_0 At/2), \quad 0 \le t < \frac{1}{N_0 A} \qquad (4.2.16)$$

$$P_k = \frac{k^{k-2}}{k!}\frac{(N_0 At)^{k-1}}{(1-N_0 At/2)} e^{-kN_0 At}, \quad 0 \le t < \frac{1}{N_0 A} \qquad (4.2.17)$$

The results of the simulations for $N_0=10^{12}$ m^{-3} and $A=1/N_0$ are shown in Figs. 4.2.3 and 4.2.4. Fig. 4.2.3 demonstrates the high degree of accuracy of the DSMC method in simulating the decrease in relative total number concentration. Here, using even only 1000 simulation particles results in very accurate results for the total number concentration. The doubling procedure is a necessity, as can be seen in Fig. 4.2.3a where the total number concentration drops with a factor of 10^3. This results in some 8 doubling procedures, clearly resulting in an accurate description. Fig. 4.2.b,c show the two other test cases. The probability distribution of aggregates with k primary particles for the above mentioned test cases is however a more sensitive function of the number of simulation particles. The statistical nature of Monte Carlo simulations become evident when there are only few aggregates in the simulation volume. This can be seen in Fig. 4.2.4a,c. where the scatter increases at large k-numbers. Fig. 4.2.4b shows clearly the decrease of the statistical scattering when increasing the number of simulation particles from 10.000 to 100.000.

a)

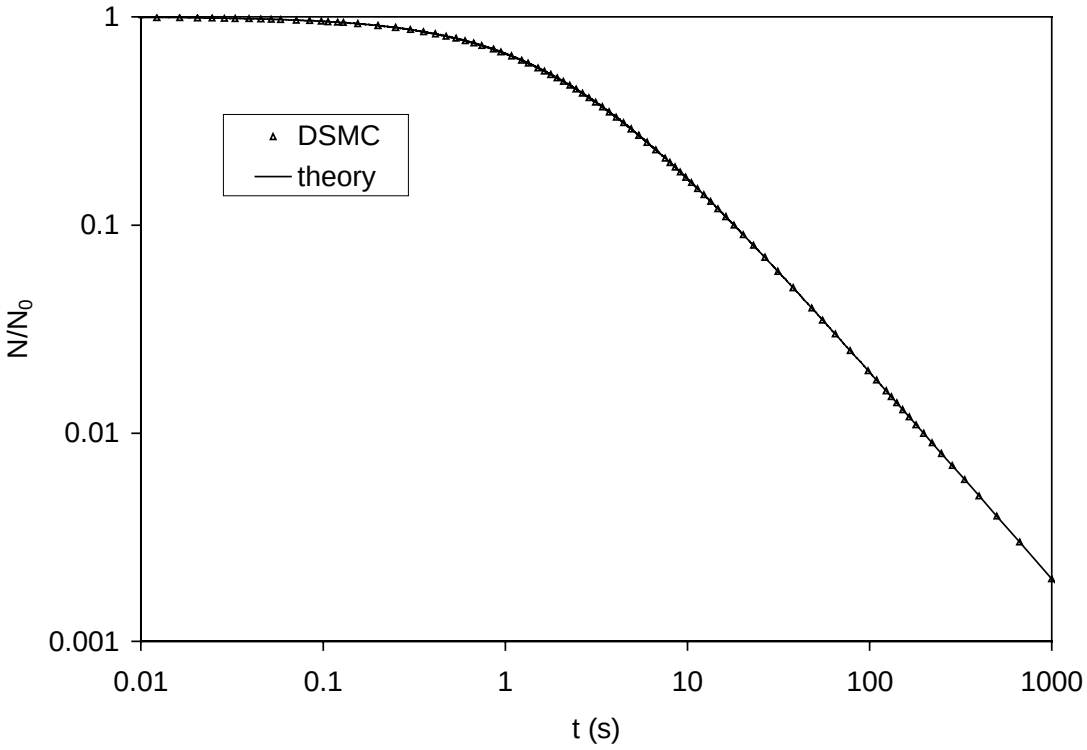
1
0.1
0.01
0.001
N/N0
DSMC
theory
0.01
0.1
1
10
100
1000
t (s)

b)

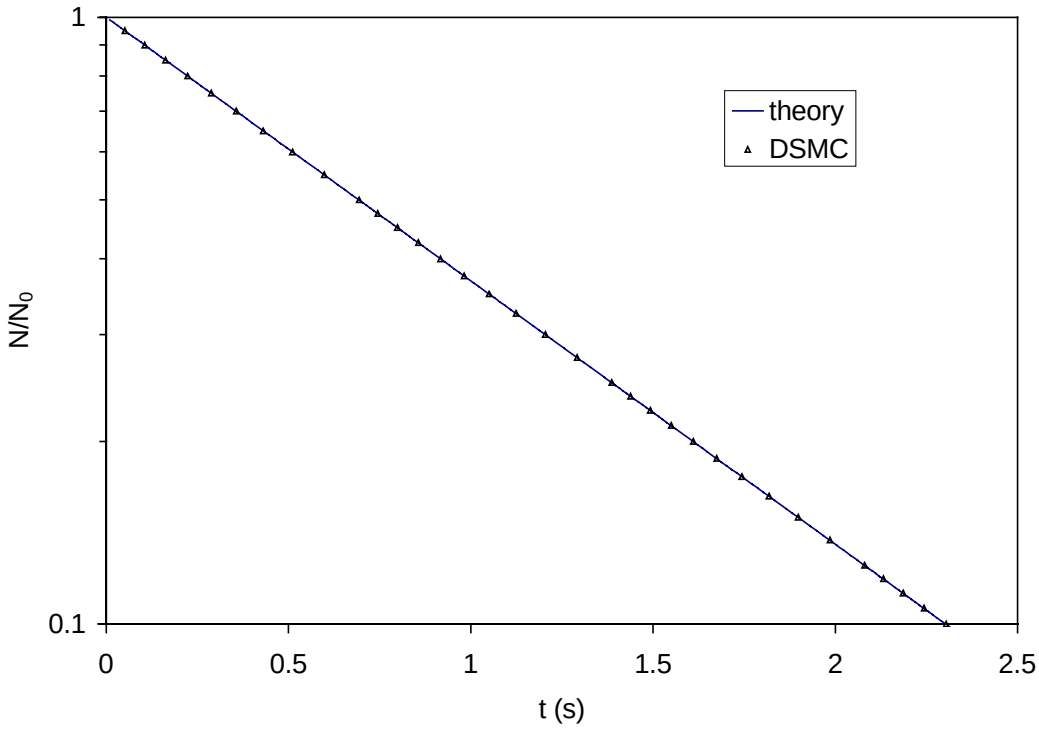
1
0.1
N/N0
theory
DSMC
0
0.5
1
1.5
2
2.5
t (s)

c)

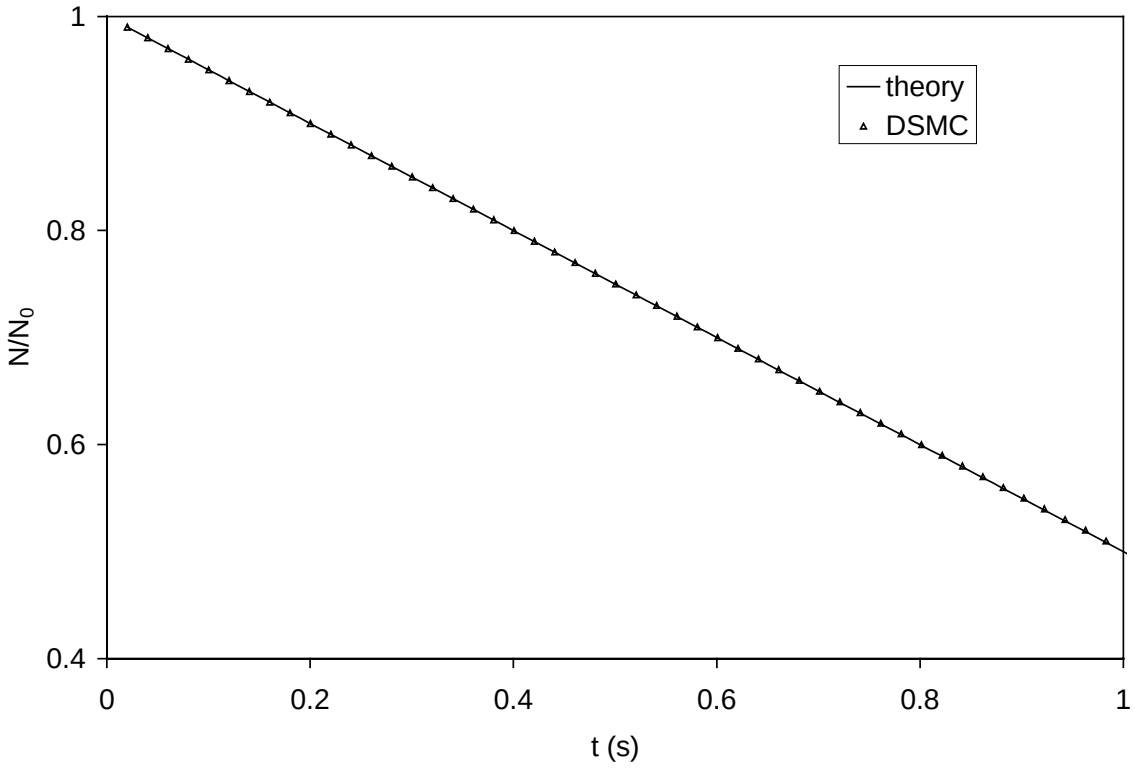

Fig. 4.2.3. Decrease in relative total number concentration N/N_0: comparison between theory and the Direct Simulation Monte Carlo method for (a) Case 1, $\beta_{i,j}=A$ (b) Case 2, $\beta_{i,j}=A(i+j)$. and (c) Case 3, $\beta_{i,j}=Aij$. Number of simulation particles: 1000.

a)

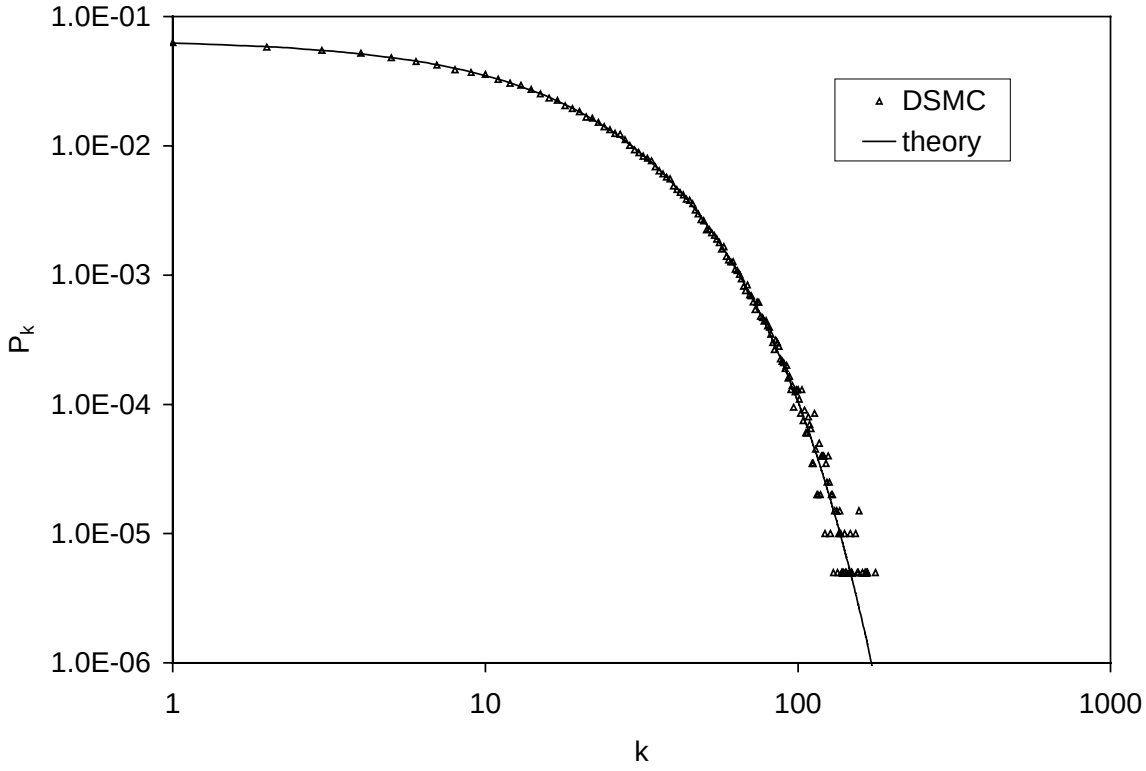
1.0E-01
1.0E-02
1.0E-03
1.0E-04
1.0E-05
1.0E-06
P_k
1
10
100
1000
k
DSMC
theory

b)

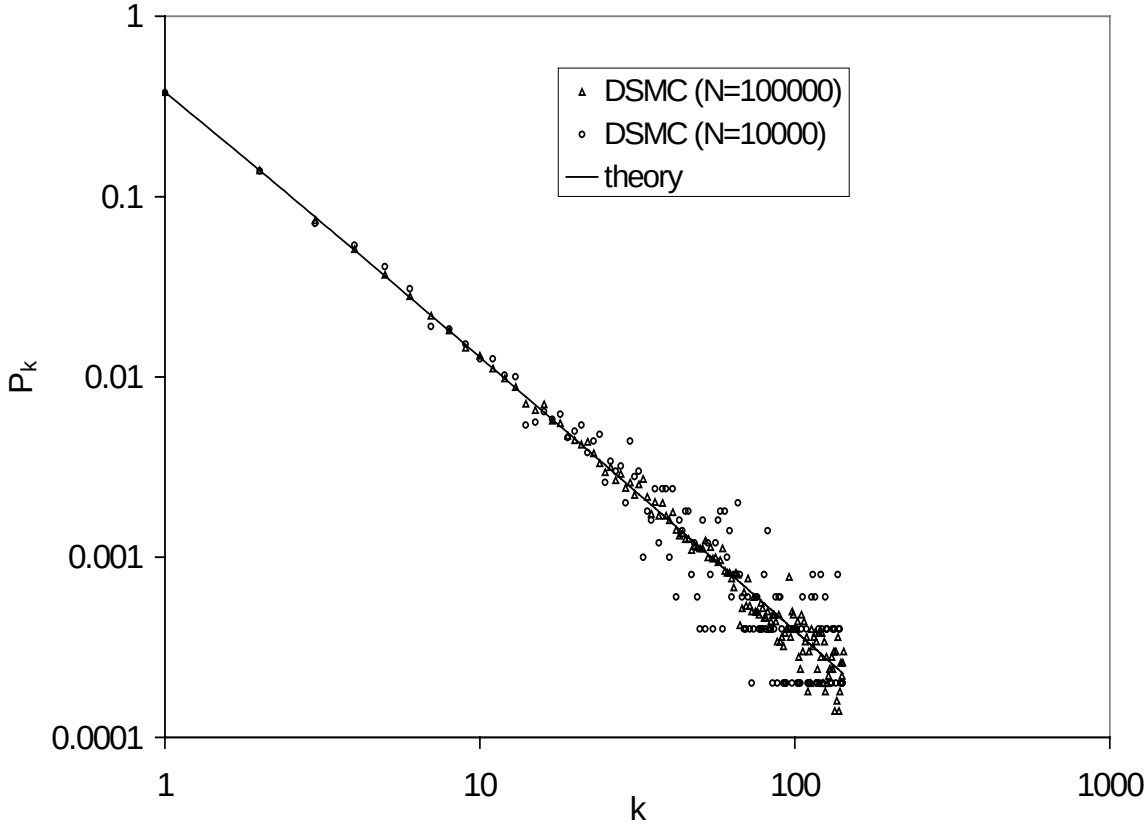
1
0.1
0.01
0.001
0.0001
P_k
1
10
100
1000
k
DSMC (N=100000)
DSMC (N=10000)
theory

c)

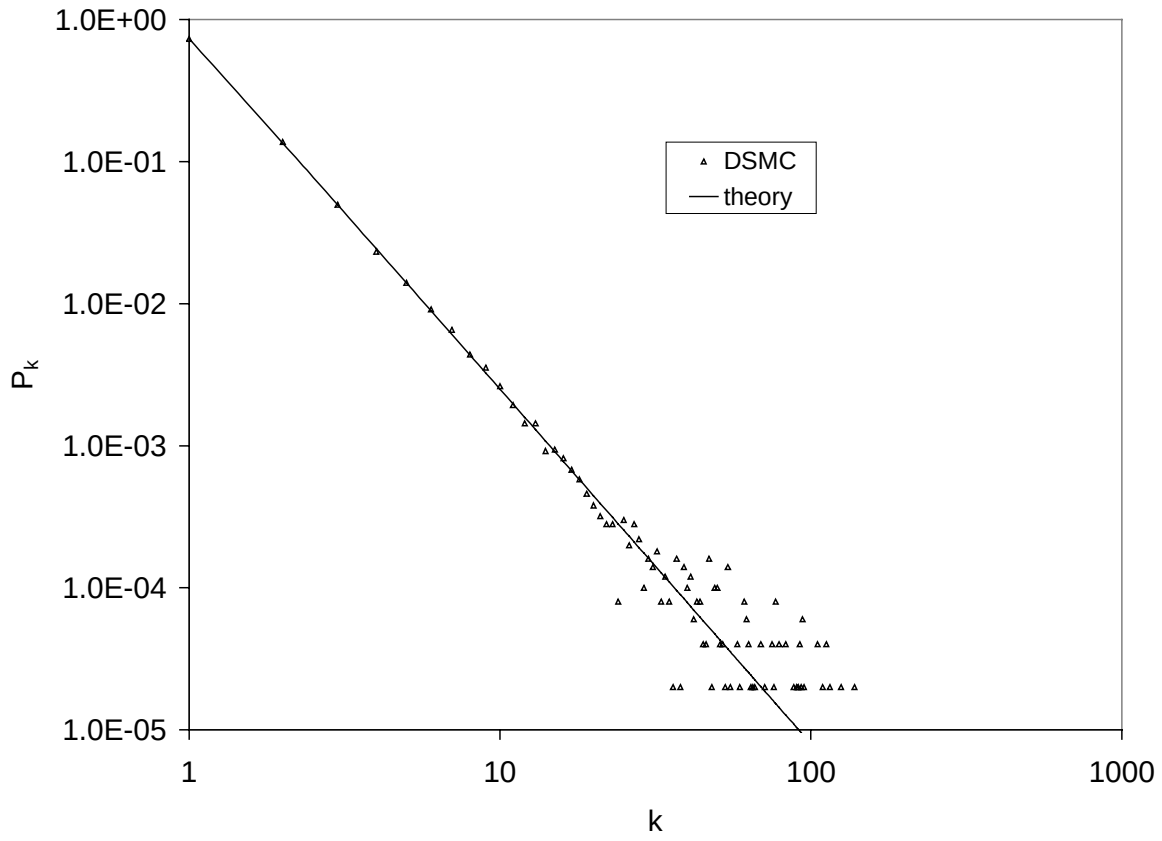

Fig. 4.2.4. The probability P_k of obtaining an aggregate containing k primary particles versus the size of the particles: comparison between theory and the DSMC method for (a) Case 1, $\beta_{i,j}=A$ at t=7.5 s (b) Case 2, $\beta_{i,j}=A(i+j)$ at t= 3.5 s and (c) Case 3, $\beta_{i,j}=Aij$ at t= 1 s. Number of simulation particles: 100.000 (a), 10.000 and 100.000 (b) and 100.000 (c).

4.2.4 Comparison with numerical solutions for coagulation

The form of the particle size distribution is an important issue in particle synthesis. In order to check the validity of the DSMC method in a more realistic system than cluster aggregation, a coagulating aerosol is simulated. In Fig. 4.2.5 the development of the geometric standard deviation σ_g in an initially polydisperse aerosol is shown. As reference a sectional model (Landgrebe and Pratsinis, 1990) is used with a section spacing of 1.08. It can be seen that two simulations with the same number of simulation particles can give different results due to the stochastic nature of the modeling. It is seen that when a sufficient number of particles is taken, the deviations to the sectional model are in the order of 1 %. As both methods are numerical it is difficult to say which one is the more correct one. The stochastic effect can be reduced by repeating the simulation with different random numbers. This is

shown in Fig. 4.2.5 for the case of 40.000 simulation particles, where the simulation now shows a smooth curve after taking the mean of 3 different simulations.

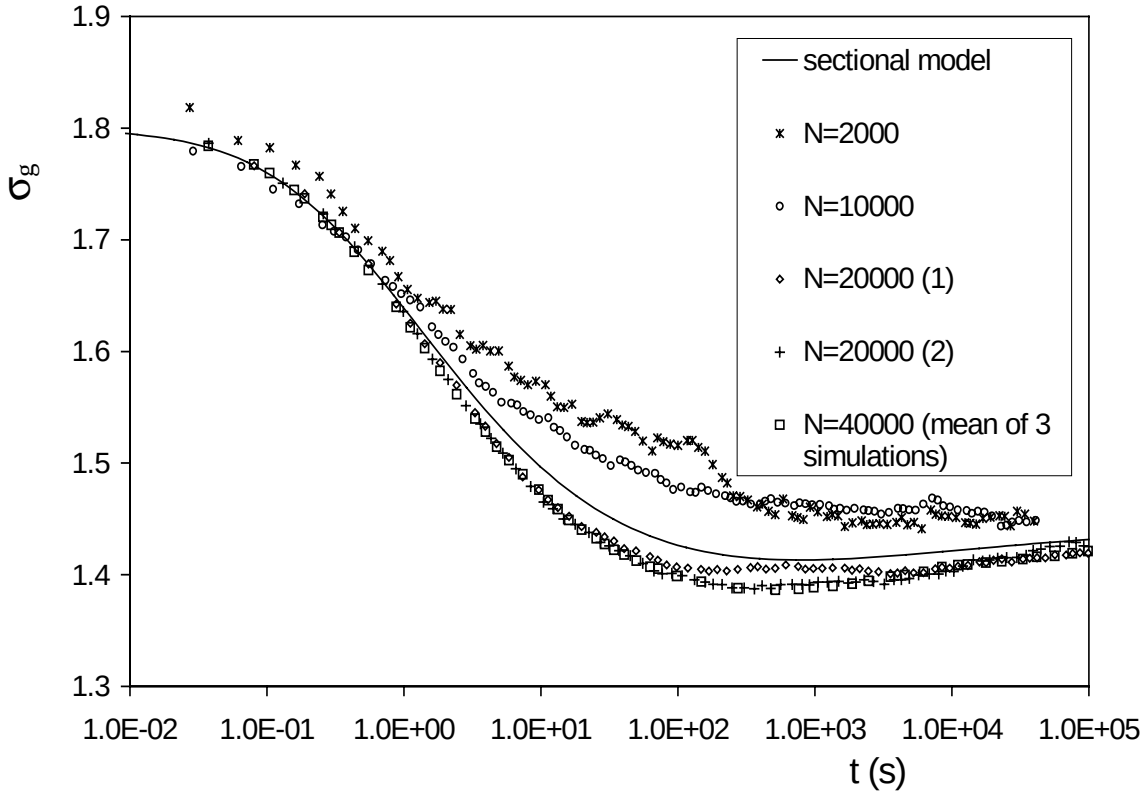

Fig. 4.2.5. The geometric standard deviation σ_g of a coagulating aerosol system (initially $d_g = 53.5$ nm, $N = 10^9\, cm^{-3}$ and $\sigma_g = 1.8$) as a function of time t: comparison between a sectional model and the DSMC method. The collision kernel used is from Dahneke (1983) and the sectional model used is by Landgrebe and Pratsinis (1990). The number of simulation particles N is indicated in the legend.

The statistic errors can be quantified by calculating the standard deviation from different simulations. This procedure is illustrated in Fig. 4.2.6, where the so-called self-preserving particle size distribution (Friedlander, 1977) for the collision kernel $\beta(v_i, v_j) = \left(v_i^{1/3} + v_j^{1/3}\right)\left(v_i^{-1/3} + v_j^{-1/3}\right)$ is shown. Ten DSMC simulations were made so that an estimation of the statistical errors could be obtained by the standard σ method (corresponding to a probability of 67 %). As can be seen from the figure, the form of the distribution is correctly described by the DSMC method and the standard σ method generally overestimates the error in the simulations. The statistical errors can be further reduced by increasing the number of simulations and/or the number of simulation particles. This was not further pursued here. Curve-fitting can also be

applied here. The most striking feature in the figure is that the left-hand side of the curve shows much larger statistical deviations than the right-hand side. This is due to the fact that the method is particle number-based: to the left of the maximum less simulation particles are available for one data point due to the logarithmic axis.

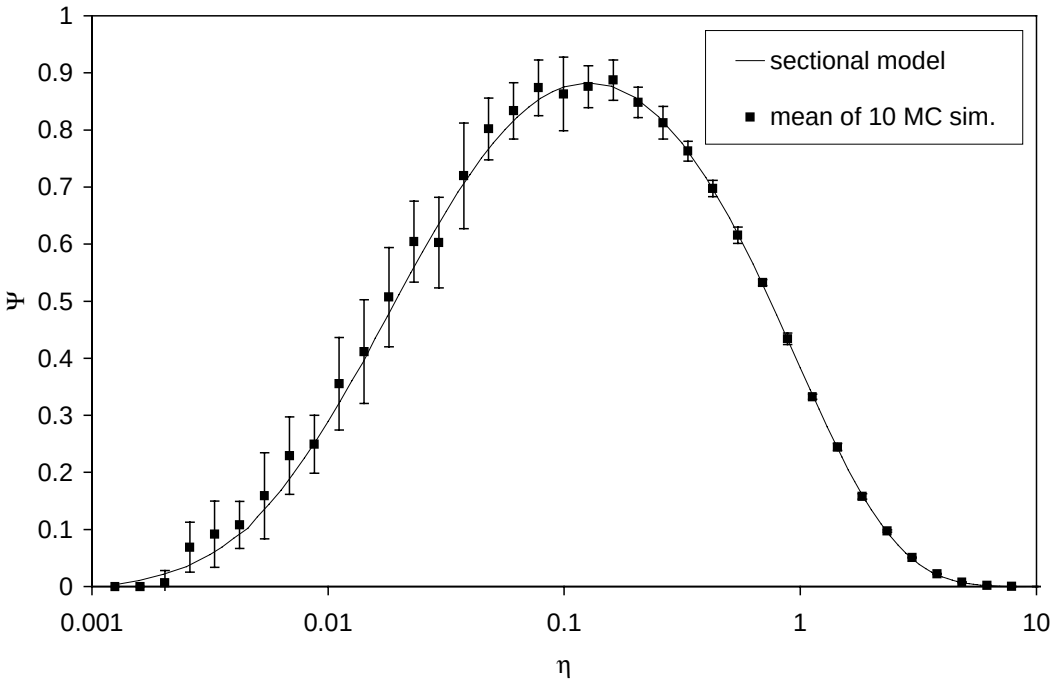

Fig. 4.2.6. Self-preserving particle size distribution for the collision kernel $\beta(v_i, v_j) = (v_i^{1/3} + v_j^{1/3})(v_i^{-1/3} + v_j^{-1/3})$*, in which the dimensionless particle density function* Ψ *(defined as* $Vn(v,t)/N^2$ *where V and N are the total particle volume and number) is a function of a dimensionless particle volume* η *(defined as* Nv/V*). The DSMC results are compared with results from Vemury et al. (1994) who use a sectional model. A confidence range of* $\pm\sigma$ *is calculated from 10 simulations.*

4.2.5 Case study 1: Chemical reaction in coagulating droplets (microreactors)

The standard numerical solution schemes, e.g. sectional models, for solving coagulating particle systems are more computer time-efficient than the DSMC simulation. They are however not very well suited for solving more complex systems such a reacting microdroplets. In order to show the applicability of the DSMC simulations, the reactive mixing of two sprays containing two different solutions is chosen. A chemical reaction takes place when droplets with solution A coagulate with droplets containing solution B, producing a new droplet acting as ‘microreactor’ in

which the product C is formed. This kind of mixing is used to mix two liquid reactants very fast. The chemical kinetics is given by:

$$\frac{\mathrm{d}[\mathrm{C}]}{\mathrm{d}t} = k\,[\mathrm{A}][\mathrm{B}] \qquad (5.2.18)$$

where $[A]$ denotes the concentration of A and k is a reaction constant. The problem is analogous with that of a chemical reaction in a liquid-liquid dispersion described by Shah *et al.* (1977). However, a polydisperse initial size distributions is used here. The chemical reaction is closely related to the droplet dynamics as a collision event changes the concentrations of the reactants and product, depending on the relative volume of the colliding droplets. The coagulation version of the DSMC code is very easily adapted for calculating the change in concentrations due to the chemical reaction between two collisions by adding only a few additional program lines.

The results of the simulation are plotted in Fig. 4.2.7. As collision kernel the collision frequency for the continuum regime (Friedlander, 1977) is taken. The results for the volume fraction of droplets *v/V* having the indicated product concentration [C] are shown in a histogram-fashion, with the values of the concentration located at the midpoint of a section. Here also several simulations were made to get an idea of the accuracy of the results by using the standard σ method. It is seen that only a few simulations are necessary to get a relative accurate result. The DSMC is an easily programmed method to calculate complicated multi-dimensional size distributions, in this case $n(v,[A],[B],[C],t)$.

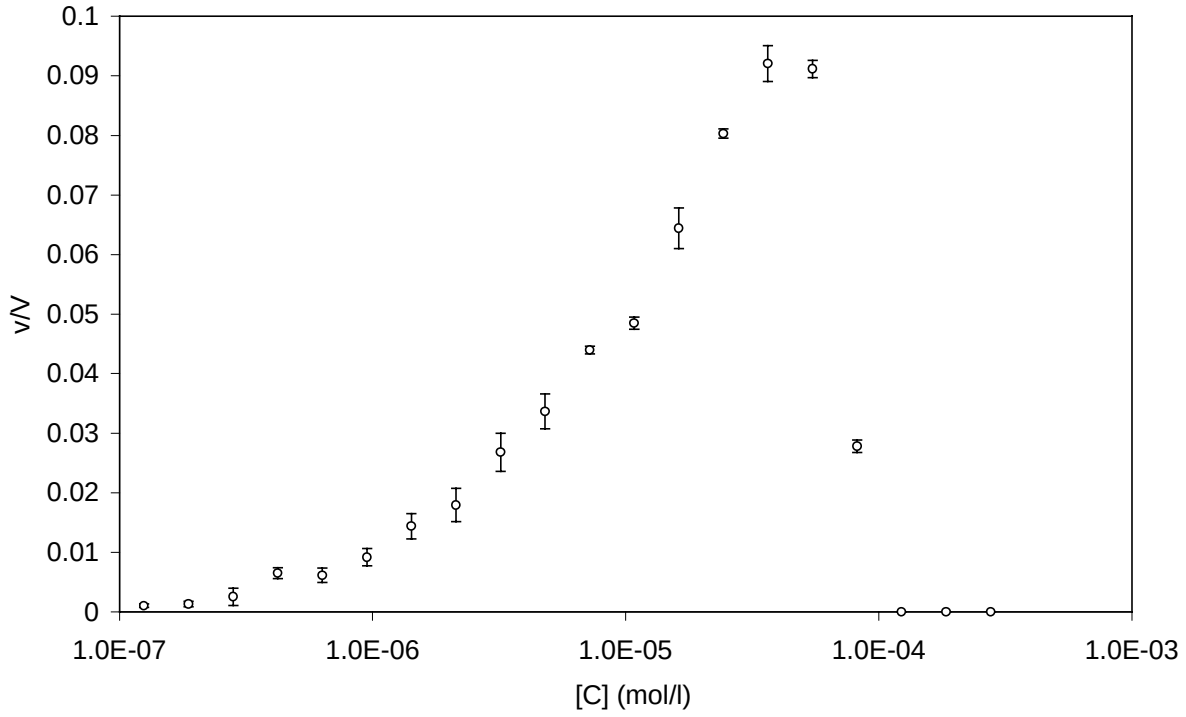

Fig. 4.2.7. Distribution of product concentration [C] resulting from the chemical reaction $A+B \rightarrow C$ with a reaction rate k=2.067 10^{-3} l/(mol s) between an A-containing spray (initially $[A]=10^{-3}$ mol/l, $d_g = 1$ µm, $N = 5\ 10^2$ cm^{-3} and $\sigma_g = 1.5$) and a B-containing spray (initially $[B]=10^{-3}$ mol/l, $d_g = 1$ µm, $N = 5\ 10^2$ cm^{-3} and $\sigma_g = 1.6$). v/V is the volume fraction of droplets having a concentration [C]. The time elapsed is 4.37 10^5 s. The initial number of simulation particles is 30.000 particles for each spray. The error bars ($\pm\sigma$) result from repeating the simulation 4 times.

4.2.6 Case study 2: Coating of particles with smaller particles by aggregation

A second example of a problem which is very difficult to solve with standard particle dynamical models is the coating of solid particles with nanoparticles with both particle fractions having an initially polydisperse size distribution. Particle coating is applied in industry to apply a functional, protective or wear-resistive layer and is often carried out in a fluidized bed reactor (Li and Hua, 1997). The problem is to determine how much of the surface of the larger particles (1 µm) is covered with the smaller particles (100 nm). This is expressed in the surface coverage, which is defined as the ratio of the sum of the area of all nanoparticles deposited on a large particle and the surface area of the large particle. Due to the polydisperse size distribution and the

random nature of the collision process, the surface coverage of the large solid particles will be a distributed variable.

For the DSMC simulation, it means that the aggregation mode has to be used where information on the primary particles composing an aggregate is stored. As an approximation, the collision kernel for the continuum regime (Friedlander, 1977) is used. The results are shown in Fig. 4.2.8 as a cumulative distribution of the surface coverage for different coating times indicated in the legend. As can be seen from the slopes of the curve, there is a rather broad distribution of surface coverage of the large particles. The results of the DSMC method are in fact a solution of the multi-dimensional size distribution $n(v_1, v_2, ..., v_{n_p}, t)$ in which n_p is the number of particles in the aggregate.

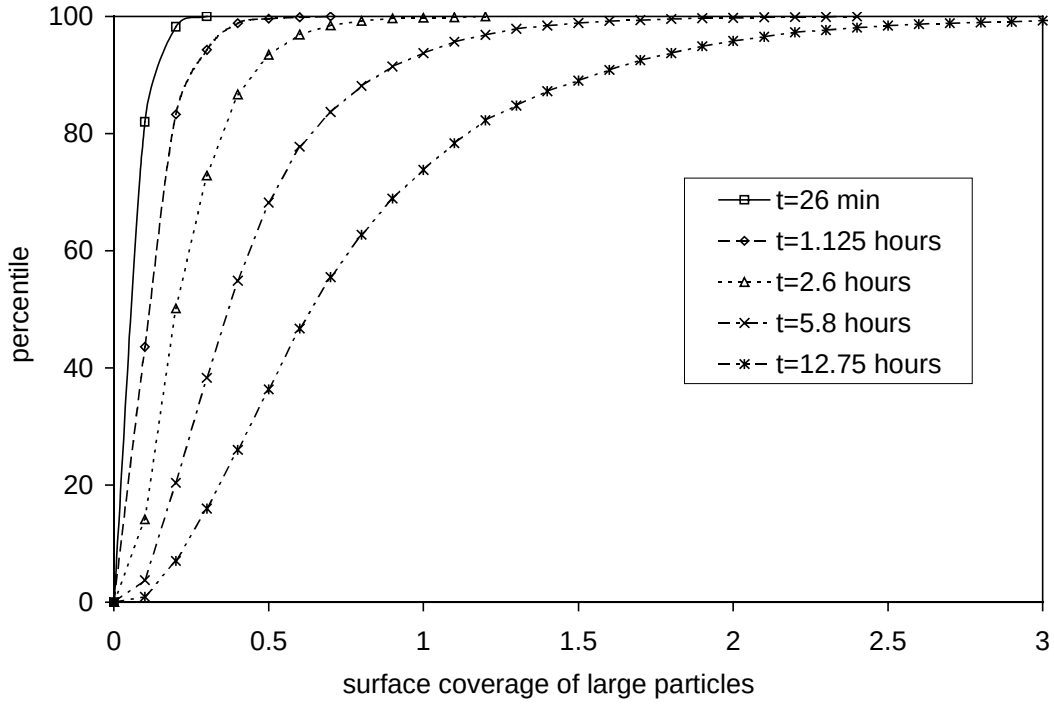

Fig. 4.2.8. Cumulative distribution of the surface coverage as a result of coating large particles ($d_g = 1$ μm, $N = 10^3 cm^{-3}$ and $\sigma_g = 1.2$) with nanoparticles ($d_g = 100$ nm, $N = 10^6 cm^{-3}$ and $\sigma_g = 1.5$) for different coating times indicated in the legend. The initial number of simulation particles is 20.000 for the nanoparticles, the simulation was repeated 5 times.

4.3 Mixing by means of aggregation of charged particles

A special case of nanomaterials is formed by composite particles, here defined as aggregates composed of two different particle classes. The technological use of such particles is manyfold, e.g.:

- improve the functional properties of semiconductor nanoparticles by adding a second semiconductor particle which provides a charge transfer, thereby improving the quantum yield,
- improve the functional properties of nanoparticles by adding another nanoparticle which has catalytic properties, such as Pt or Pd which enhances the sensitivity of SnO_2 nanoparticles used for gas sensors,
- improve the superconductive properties of YBCO particles by adding smaller particle which act as flux pinning enhancement (Takao *et al*., 1997),
- improve the mixing characteristics when two ultrafine powders have to be mixed: when the powders are mixed in aerosol form, the occurance of large aggregates of one component, which is detrimental for the mixing, can be suppressed.

When mixing of primary particles of different chemical composition (e.g., component A and B) takes place by Brownian coagulation, the mixing is a stochastic process in which as many aggregates composed of two A particles will occur as composite particles A-B when both particle components have the same size. The mixing quality can be enhanced by applying electrical forces. When the two particle components are oppositely charged, it is clear that more well-mixed A-B composite particles will be obtained than unmixed doublets of A or B (Fig. 4.3.1).

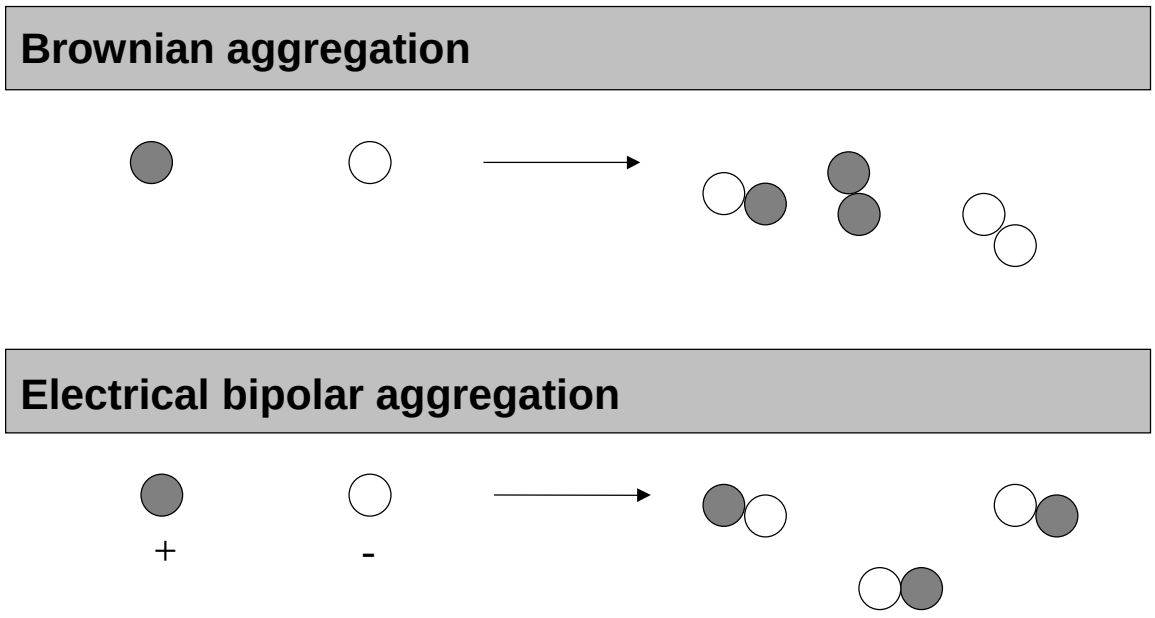

Fig. 4.3.1. Principle of influencing aggregate formation by charges on particles.

The dynamic behavior of such systems is complicated, because the aggregates formed may consist of particles dissimilar with respect to size, electrical charge and composition. Numerical techniques have to be applied in order to simulate the dynamical behavior when no assumptions about the form of the particle size distribution are made. These techniques, such as the sectional model (Gelbard *et al*., 1980), require complicated programs. The addition of charges further complicates these models. Oron and Seinfeld (1989) developed a detailed but very elaborate sectional model for the dynamics of charged particles, necessitating the solution of the two-dimensional distribution $n(v,q)$ as a function of time. Vemury *et al.* (1997) used the simpler sectionalization technique developed by Litster *et al.* (1995). Even when simplifying assumptions such as a log-normal shape of the size distribution and a fixed charge distribution are made (Otto, 1997), the mathematical description remains very cumbersome. Models involving charge and size have mainly been applied for describing the charging of particles by ions and the increase in mean particle size by bipolarly charging an aerosol which has to be precipitated (Otto *et. al*., 1996).

Several studies considered the coagulation of two- or multi-component aerosols. Lushnikov (1976) was the first to consider the coagulation of two-component mixtures, deriving an analytical solution for a size-independent coagulation kernel. Gelbard and Seinfeld (1980) developed a sectional technique for dynamic behavior of particle size and chemical composition. However, both the setting up of the kinetic equations and their numerical solution are very time-consuming. Another numerical technique for dealing with two-component coagulation was independently developed by Piskunov *et al.* (1997). These models have mainly been applied to atmospheric aerosols, e.g. to account for chemical reactions in water droplets or to describe accidental release of radioactive species and their deposition onto aerosols. At present, however, no models exist for simultaneously solving the size, electrical charge and composition of an aerosol.

In this subchapter, we investigate what are optimal conditions for obtaining composite particles containing the same number of primary particles of the different components. When a large fraction of such agglomerates is present, the primary particles can be considered as well mixed. We consider several possible methods: the mixing of bipolarly charged aerosols, the mixing of unipolarly charged aerosols and the laboratory method of mixing size-selected and oppositely charged nanoparticles. The use of the newly developed DSMC technique (Chapter 4.2.) allows us to obtain insight in the behavior of these complicated processes, in which the formed particles are in the form $A_i B_j$ (with $i,j \geq 0$) and where the primary particles have a size and charge distribution.

4.3.1 Theory of bipolar aggregation

For the case of spherical uncharged particles, Fuchs (1964) proposed an interpolation formula for the coagulation coefficient valid in the whole particle size range:

$$\beta_{i,k} = 2\pi D_{i,j}(d_i + d_j)\left(\frac{d_i + d_j}{d_i + d_j + 2\delta_{i,j}} + \frac{8D_{i,j}}{\bar{v}_{i,j}(d_i + d_j)}\right)^{-1} \qquad (4.3.1)$$

with

$$\delta_{i,j} = \sqrt{\delta_i^2 + \delta_j^2}\ ,\ \delta_i = \left(\frac{1}{3d_i\lambda_i}\right)\left((d_i + \lambda_i)^3 - (d_i^2 + \lambda_i^2)^{\frac{3}{2}}\right) - d_i \qquad (4.3.1a)$$

$$\lambda_i = \frac{8D_i}{\pi\bar{v}_i} \qquad (4.3.1b)$$

$$\bar{v}_i = \sqrt{\frac{8k_BT}{\pi m_i}} \qquad (4.3.1c)$$

$$\bar{v}_{i,j} = \sqrt{\bar{v}_i^2 + \bar{v}_j^2} \qquad (4.3.1d)$$

$$D_i = \frac{Ck_BT}{3\pi\eta d_i} \qquad (4.3.1e)$$

$$D_{i,j} = D_i + D_j \qquad (4.3.1f)$$

where m is the particle mass, k_B is the Boltzmann constant, T is the fluid temperature, η is the dynamic gas viscosity, d is the particle diameter, C is the slip correction factor, and the indexes i and j refer to the colliding particles. Different particle densities of the colliding particles are taken into account by this formula. If the particles are charged, the Coulomb forces have to be considered and the coagulation coefficient has to be corrected into:

$$\beta_{i,j;el} = \frac{\beta_{i,j}}{W_{i,j}^{p,q}}\ , \qquad (4.3.2)$$

where $W_{i,j}^{p,q}$ is the Fuchs stability function (Fuchs, 1964):

$$W_{i,j}^{p,q} = -\frac{1-\exp(\kappa)}{\kappa} \qquad (4.3.2a)$$

$$\kappa = \frac{2pqe^2}{4\pi\varepsilon\varepsilon_0(d_i + d_j)k_B T} \qquad (4.3.2b)$$

where p and q are the numbers of elementary charges on particles i and j, respectively. This correction factor $1/W_{1,2}^{p,q}$ is shown in Fig. 4.3.2 for singly charged nanoparticles. It can be seen that this correction becomes important for smaller particles.

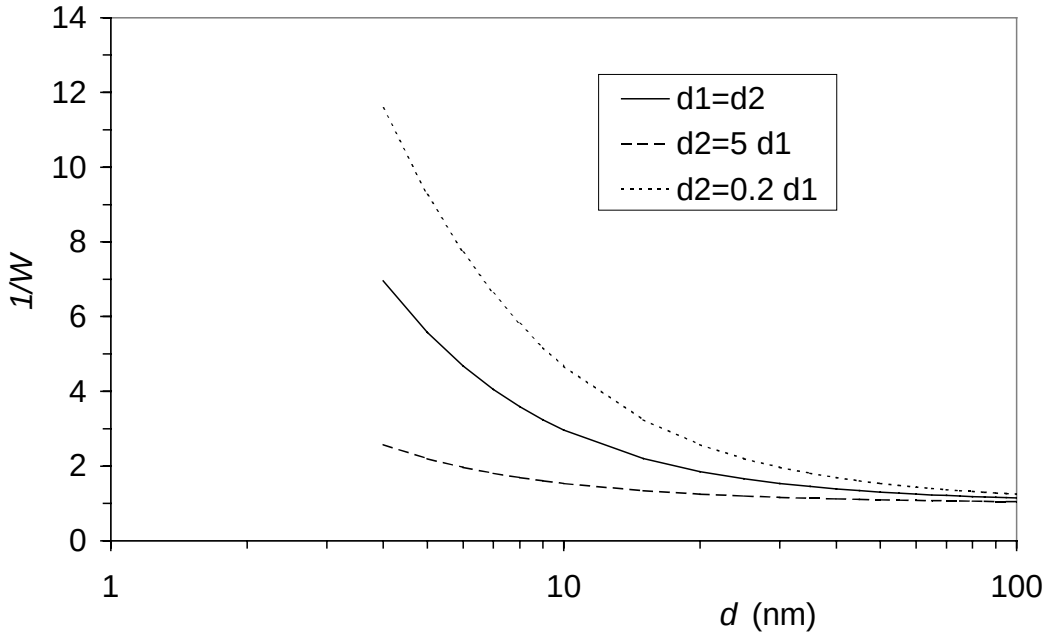

Fig. 4.3.2. Correction factor $1/W_{1,2}^{p,q}$ *for the influence of opposite charges (p= -1, q= 1) on two coagulating particles*

Furthermore, it is important to take into account in the calculation of the coagulation coefficient that the aggregates formed are not any more spherical, in contrast to the primary particles. This leads to a higher coagulation coefficient in comparison to the case when the new particle has again a spherical shape (Katzer *et. al.*, 1998). A commonly used correction method is to describe the effective aggregate diameter d by means of a fractal dimension D_f (Matsoukas and Friedlander, 1991):

$$\left(\frac{d}{d_0}\right)^{D_f} = N_p, \qquad (4.3.3)$$

in which N_p is the number of primary particles with diameter d_0. This method is, however, only applicable for equal-sized primary particles. To overcome this problem the effective diameter of an aggregate composed of primary particles of any size is estimated by calculating the projected outer diameter and taking the mean over all possible orientations. By comparing the results with the expression of Matsoukas and Friedlander for the effective aggregate diameter *d* (1991), eq. (5.3.3), the methods are found to be equivalent for D_f =1.43. Smaller fractal dimensions are encountered only for magnetic particles which tend to align. In order to be able to describe the aggregation process for higher fractal dimensions, we simply interpolate between this lower boundary and the densest possible aggregate with a D_f =3.

4.3.2 Simulation of aggregation of charged aerosols for mixing purposes

With the coagulation coefficient for charged particles and aggregates composed of unequal-sized primary particles now being known, the dynamics of the aggregation process can be studied by means of the DSMC method described in Chapter 4.2. . The simulations are performed for a bicomponent mixture with equal number concentrations of both components ($N_A = N_B$). The number of simulation particles is 20000. Each simulation was repeated five times with different random numbers to reduce the influence of the stochastic nature of the simulation process. Mean values were computed from these five simulations. Each component has an initial lognormal size distribution, which is also generated by means of random numbers (Rubinstein, 1981). The initial charge distribution can be based on any formula for the charging method used, such as bipolar charging or unipolar charging. The bipolar charge equilibrium for particles larger than 50 nm can be described by the Boltzmann charge distribution, where the concentration ratio of particles carrying *q* elementary charges is (Fuchs, 1964):

$$\frac{N^q}{N^0} = \exp\left(-\frac{q^2}{2\sigma^2}\right) \tag{4.3.4}$$

where N_0 is the total particle number and with

$$\sigma = \sqrt{\frac{dk_B T}{2e^2}} \tag{4.3.5}$$

As the Boltzmann theory underestimates the number of charged particles with diameters smaller as 50 nm, the following approximation formula is used (Wiedensohler, 1988):

$$F(q) = 10^{\sum_{i=0}^{5} a_i(q) \log \frac{d}{nm}} \qquad (4.3.6)$$

where *F(q)* is the distribution function and $a_i(q)$ are coefficients as determined by Wiedensohler.

The aerosols investigated have initial geometric mean diameters d_g in the 10 to 100 nm range. For smaller nanoparticles it is more difficult to reach sufficiently high charge levels for influencing the aggregation process, and they were therefore not considered. The aggregates which were formed were assumed to have a fractal dimension D_f =1.43. The same initial number concentrations are used in all the cases, $N_{A,\,t=0} = N_{B,\,t=0} = 5 \times 10^5$ cm^{-3} in order to be able to compare the results for different cases. Higher or lower values of these values only influence the kinetics of the mixing process, not its qualitative behavior. Particle densities were taken to be 7500 kg/m^3 and 9600 kg/m^3 for aerosols A and B, respectively. As carrier gas N_2 at 20°C was taken.

The simulation results in a complex mixture which consist of the number concentrations of $A_i B_j$ aggregates containing primary particles with different sizes and charges. The mixing quality can be shown by means of the distribution function. The distribution function of primary particles $N_{i/(i+j)}/N$ is based on the ratio of the number of primary particles of one component to the total number of primary particles in the aggregate, $i/(i+j)$. Here, *i* corresponds to the number of primary particles of component A and *j* refers to the primary particles of component B. In Fig. 4.3.3 an example is given of the time evolution of the distribution function of primary particles in the case of two bipolarly charged aerosols with mean particle diameters of 10 nm.

The initial unmixed situation shows two peaks, indicating the unaggregated primary particles. At the half time $t_{0.5}$ (689 s) maximum values at $i/(i+j)$ = 33, 50 and 66 % develop, representative for $A_{2n}B_n$, A_nB_n and A_nB_{2n} aggregates. At longer times larger and more complex aggregates develop, but there is still a maximum around symmetric aggregates.

In order to simplify the representation of the results, another definition is used here. The number fraction of symmetric aggregates N_{sym}/N represents the fraction of symmetric $A_i B_{j=i}$ aggregates, which corresponds to perfectly mixed aggregates. In some way N_{sym}/N is an indication of the mixing selectivity.

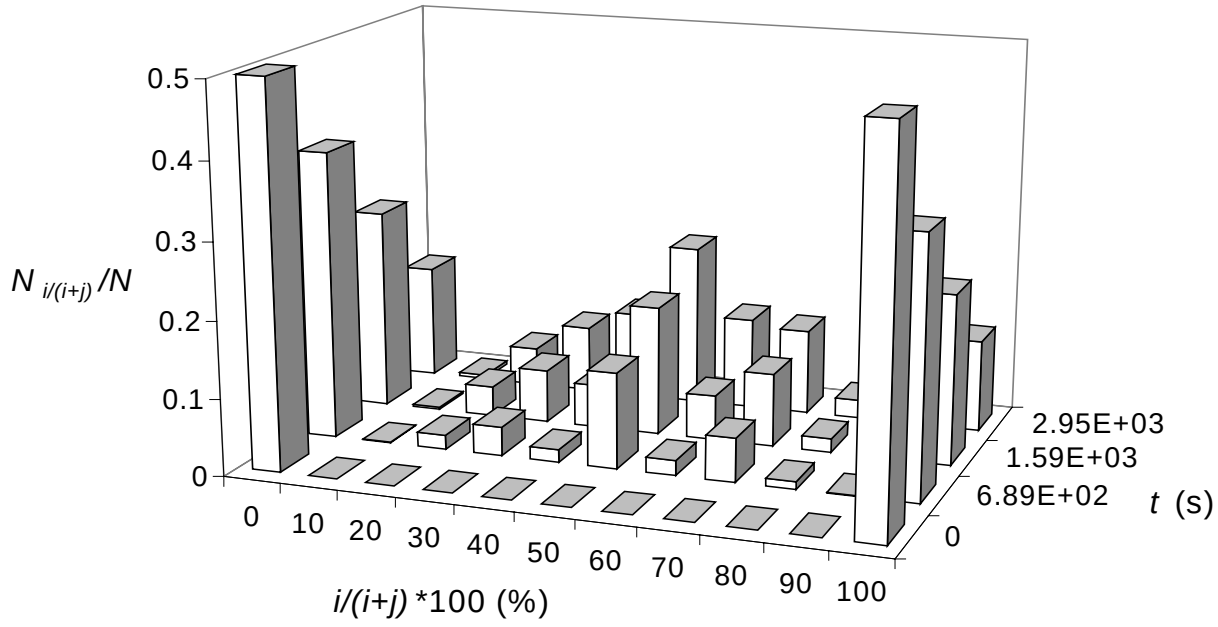

Fig. 4.3.3. Time-dependent distribution function of primary particles in aggregates. Initial conditions are $d_{g,A}$ *= 10 nm,* $d_{g,B}$ *= 10 nm,* $\sigma_{g,A}$ *=1.8 and* $\sigma_{g,B}$ *=1.6. Both aerosols are initially bipolarly charged*

4.3.3 Results

In order to assess different methods which can be used to obtain composite particles, we investigated three cases. These are: the mixing of bipolarly charged aerosols, the mixing of unipolarly charged aerosols and the laboratory method of mixing size-selected and oppositely charged nanoparticles.

The mixing of bipolarly charged particles is representative of the mixing of aerosols which are in charge equilibrium. The charge equilibrium is obtained after conducting the aerosol through a radioactive source, often used to obtain a known charge distribution or to minimize the charge level of charged aerosols. Consequently, both aerosols contain neutral particles and charged particles of both polarities. Aerosols with broad size distributions were used in the simulation, with σ_g =1.8 and σ_g =1.6 for the aerosol with component A and B, respectively. The time evolution of the number fraction of symmetric aggregates N_{sym}/N is important to find the optimal conditions for such mixing processes. From Fig. 4.3.4a it becomes clear that N_{sym}/N becomes larger with increasing particle size difference, but does not exceed 0.25. The decrease after some longer time can be explained by the formation of a wide range of aggregate which are not exactly symmetric.

Charging of aerosols in radioactive neutralizers has some drawbacks: the charging efficiency is relatively low and the bipolar nature of the charge distribution

decreases the selectivity of the aggregation process. Unipolar chargers applying an alternating electric field (Büscher *et al.*, 1994, Kruis *et al.*, 1998) allow to solve these problems. They possess a higher charging efficiency than radioactive neutralizers as they are not limited by the bipolar charge equilibrium, and all charges are of one sign. Therefore, mixing unipolar aerosols can be more suitable for industrial application. For our simulations, aerosols with the same particle size distribution function as for bipolar charged particles ($\sigma_{g,A}$=1.8, $\sigma_{g,B}$=1.6) were used, but this time one of them contains only positively charged particles (A), and the other (B) contains only negative charges with some amount of uncharged particles in both aerosols. Charging efficiencies in both aerosols are taken similar to those described by Büscher *et al*. (1994) for positively charged particles. The increased fraction of charged particles as compared to the bipolar case and the fact that particles of different kinds carry only charges of opposite signs have a positive influence on the fraction of symmetric aggregates, as can be seen from Fig. 4.3.4b. Remarkable is not only an increase of N_{sym}/N of roughly a factor 2 with respect to bipolarly charged aerosols, but also different conditions leading to a maximum of selectivity. It was found that the maximum of N_{sym}/N is for both aerosols having the largest diameters. This is due to the competition of two effects: on the one hand the coagulation coefficient increases with increasing difference in particle sizes, on the other hand for larger particles the correction factor due to electric charge strongly increases due to the multiple charges. Clearly, the first effect dominates in case of bipolarly charged aerosols due to a low fraction of multiple charged particles while in case of unipolarly charged aerosols the second effect prevails.

Comparison of the results for the bipolar and unipolar cases leads to recognition of the importance of the number and sign of charges on particles for the aggregation process. For further study a bicomponent mixture of particles with a narrow size distribution (σ_g=1.1) carrying an equal charge number but of opposite sign (q_A=-q_B) was taken. These aerosols can be obtained using the standard equipment for particle fractionation consisting of an aerosol charger and a Differential Mobility Analyzer. For applications, however, it has one main disadvantage: the maximum particle number concentration which can be obtained is relatively low. The evolution of N_{sym}/N, representing the selectivity, is presented in Fig.4.3.4c for $d_{g,A} = d_{g,B}$= 30 nm. The maximum charge level is taken to be three elementary charges, as this is the limit for the diffusion charging for 30 nm sized particles according to Fuchs (1963). It can be seen that only multiply charged particles result in high selectivity, over 80 % for triply charged particles. It was found in simulations not shown here that the highest selectivity is obtained for the smallest particle sizes and the highest charge levels taken. This is due to the fact that all particles are charged and to the higher mobility of smaller particles.

a)

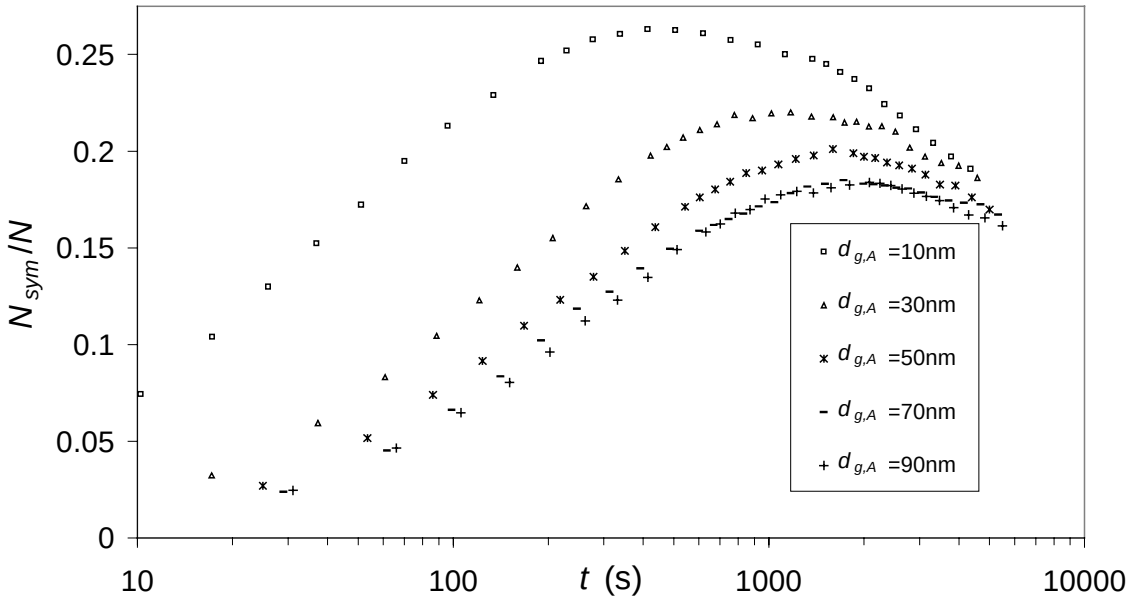
0.25
0.2
0.15
0.1
0.05
0
N_{sym}/N
10
100
t (s)
1000
10000
$d_{g,A}$ =10nm
$d_{g,A}$ =30nm
$d_{g,A}$ =50nm
$d_{g,A}$ =70nm
$d_{g,A}$ =90nm

b)

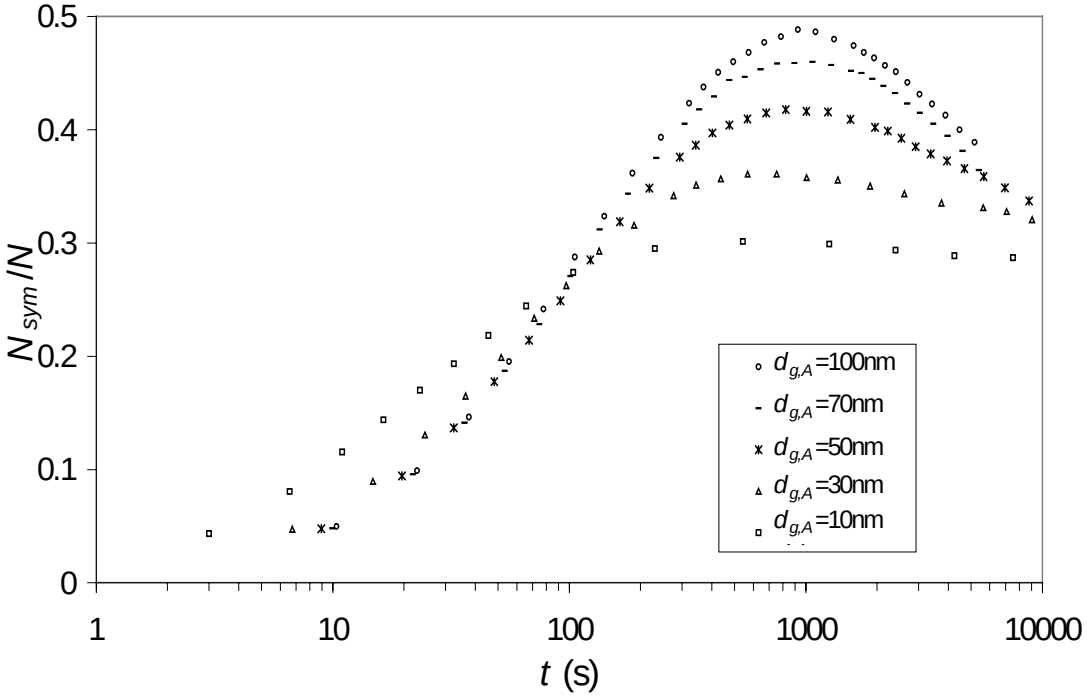
0.5
0.4
0.3
0.2
0.1
0
N_{sym}/N
1
10
100
1000
10000
t (s)
$d_{g,A}$=100nm
$d_{g,A}$=70nm
$d_{g,A}$=50nm
$d_{g,A}$=30nm
$d_{g,A}$=10nm

c)

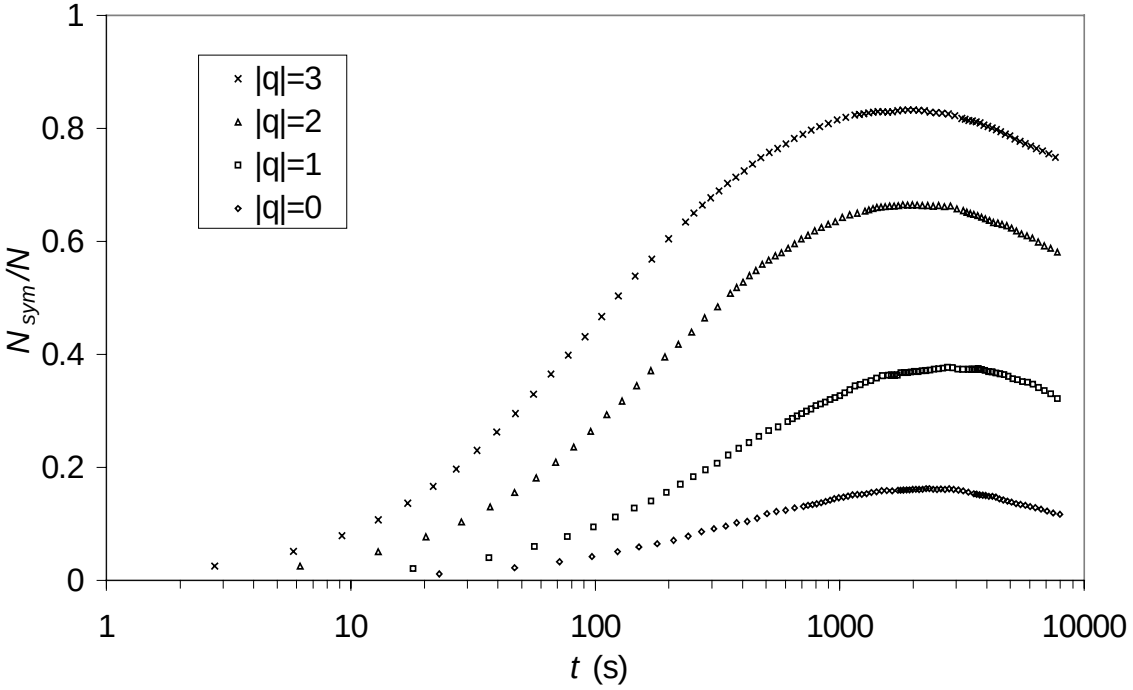

Figure 4.3.4. Fraction of "symmetric" aggregates as function of time: a) in the case of initially polydisperse bipolarly charged (according to Wiedensohler, 1988) primary particles for different mean geometric diameters of component A with $d_{g,B}$=90 nm, b) in the case of initially polydisperse unipolarly charged (according to Büscher et al., 1994) primary particles for different mean geometric diameters of component A with $d_{g,B}$=90 and c) in the case of initially quasi monodisperse ($d_{g,B}=d_{g,A}$=30 nm) oppositely charged ($q_A=-q_B$) primary particles for different charge levels.

4.4 Conclusions: mechanisms relevant for gas-phase synthesis

The formation of nanoparticles by the evaporation-condensation technique was analyzed using a moment model describing nucleation, condensation and coagulation. Using the model, it was shown that the temperature in the evaporation furnace and the cooling rate determines the mean particle size and that an aerosoldynamical model allows the prediction of the temperatures needed for nanoparticle formation. For obtaining particle in the nanometer size-range, a temperature range of some 200-300 K can be found for each element. In the Chapters 7.1 and 7.2 the evaporation-condensation technique is experimentally applied.

For more complicated systems having more degrees of freedom, such as distribution of particle sizes, different chemical compositions, distribution of charges and distribution of number of primary in an aggregate, a newly developed Direct Simulation Monte Carlo method showed to be suitable. Two examples of practical relevance containing multi-dimensional particle dynamics were given: coagulation with chemical reaction in droplets (microreactors) and the coating of solid particles with nanoparticles.

Aggregation of mixtures of charged nanoparticles is useful for obtaining composites. This was studied by means of the Direct Simulation Monte Carlo method. The selectivity of mixing is characterized by means of the fraction of symmetric aggregates. It was shown that for each charge distribution different conditions lead to a highest possible selectivity. Chapter 7.4 will describe an experiment designed for obtaining very well-defined composite nanoparticles, based on charges on nanoparticles.